Flow Behavior of Two Side-Chain Liquid Crystal Polymers Studied by Transient Rheology

Isabel Quijada-Garrido,[†,§] Hartmut Siebert,[†] Christian Friedrich,[‡] and Claudia Schmidt*[,†]

Institut für Makromolekulare Chemie, Albert-Ludwigs-Universität Freiburg, Stefan-Meier-Strasse 31, D-79104, Freiburg, Germany, and Freiburger Materialforschungszentrum (FMF), Albert-Ludwigs-Universität Freiburg, Stefan-Meier-Strasse 21, D-79104, Freiburg, Germany

Received August 31, 1999; Revised Manuscript Received March 10, 2000

ABSTRACT: Transient stresses in shear-rate-controlled experiments were measured for two nematic side-chain liquid crystal polymers (side-chain LCPs), a flow-aligning one and a non-flow-aligning one, over a range of different temperatures. The chemical structures of the LCPs differ in the number of methylene groups in the spacer linking the mesogenic side groups to the polysiloxane backbone. The LCP with the shorter spacer forms only a nematic liquid crystalline phase and is flow-aligning over the whole temperature range of this phase. In contrast, the LCP with the longer spacer has an additional low-temperature smectic phase and is a non-flow-aligning nematic. Damped time-dependent oscillations in both the first normal stress difference and the shear stress were found for the non-flow-aligning side-chain LCP, whereas a rheological response characteristic of a flow-aligning system was found for the other one. A comparison of the oscillating transients of the non-flow-aligning LCP with Ericksen's transversely isotropic fluid model shows good agreement for the shear stress but not for the first normal stress difference. The intensity of the stress oscillations in the non-flow-aligning system increases spectacularly after prior squeezing or stretching of the sample. Its rheological response after flow reversal is in agreement with the previously observed "log-rolling" orientation of the mesogens. In the range of shear rates studied, both polymers are slightly shear thinning and show positive steady-state values of the first normal stress difference, which increases almost linearly with increasing shear rate.

1. Introduction

The flow behavior of liquid crystal polymers (LCPs) is more complex than that of simple polymers because LCPs are anisotropic fluids.[1−4] Thermotropic LCPs, in contrast to lyotropic ones, exhibit a liquid crystalline phase in the bulk state. There are two main types of thermotropic LCPs. The mesogen can be incorporated along the polymer backbone, resulting in main-chain LCPs, or the LCP is built of a flexible polymer chain to which the mesogenic groups are attached as side chains through a flexible spacer. The latter are called side-chain LCPs. The spacer is introduced in order to decouple the antagonistic ordering tendencies of the backbone and the mesogen. In main-chain LCPs the dynamics of the mesogen and the backbone remain strongly coupled, and the spacer merely increases the flexibility of the backbone. In side-chain LCPs the decoupling makes the mesogens more mobile and field active. Therefore, the rheological response of these two kinds of thermotropes is expected to be different.

Among the interesting flow phenomena that can be observed in LCPs is the tumbling instability of nematics. The Leslie−Ericksen−Parodi theory predicts two classes of nematics that can be characterized by the value of the reactive parameter $\lambda = (\alpha_2 + \alpha_3)/(\alpha_2 - \alpha_3)$, expressed here in terms of the Leslie viscosity coefficients α_i.[1,5] The first type of nematics, the non-flow-aligning or tumbling type, comprises materials with $|\lambda| < 1$. In this case, the nematic director is forced by the hydrodynamic torques to rotate continuously in a simple shear flow. For the second type, the flow-aligning type, characterized by $|\lambda| \geq 1$, the director adopts a stable orientation at a characteristic angle, the Leslie angle, with respect to the flow direction.

The tumbling instability has been found responsible for some unusual rheological properties of nematic LCPs, such as a negative first normal stress difference (N_1) and transient oscillations of N_1 and shear stress (σ) at moderate shear rates ($\dot{\gamma}$).[1−4,6] Onogi and Asada[7] distinguish three flow regions with different dependence of the viscosity (η) on the shear rate: region I, at low shear rates, showing shear thinning; region II, at intermediate shear rates with a Newtonian plateau; and at higher shear rates region III, again showing shear thinning. This behavior has been observed experimentally for several LCPs.[1−4,8] Negative values of the first normal stress difference appear near the crossover from region II to region III.

Some efforts have been made to understand this peculiar behavior. Calculations that predict the director orientation and the rheological response of a nematic LCP under flow are based mainly on the molecular theory for concentrated solutions of rodlike molecules by Doi.[9] Marrucci and Maffetone[10] calculated the predictions of the Doi theory for a two-dimensional model. The molecules were assumed to lie in the plane defined by the velocity and the velocity gradient. With this simplification, they were able to predict tumbling at low shear rates, and a transition from tumbling to flow-aligning as well as the region of negative values of N_1 that occur when the shear rate is high enough to distort the orientational distribution function, making it less anisotropic. Larson[11] considered the problem in three

† Institut für Makromolekulare Chemie.
‡ Freiburger Materialforschungszentrum (FMF).
§ Present address: Instituto de Ciencia y Tecnología de Polímeros, Juan de la Cierva 3, E−28006, Spain.
* Corresponding author: Telephone +49-761-203 6314; Fax +49-761-203 6306; E-mail schmidtc@ruf.uni-freiburg.de.

10.1021/ma991490m CCC: $19.00
Published on Web 04/27/2000

dimensions, allowing molecular orientation in the vorticity direction. He confirmed the main conclusions of Marrucci and Maffetone[10] but predicted an additional transition region between tumbling and flow-aligning where the director wags between two different directions. More recent calculations by Larson and Öttinger[12] predicted out-of-plane solutions that can be either the log-rolling state, that is, a stable orientation parallel to the vorticity axis, or kayaking orbits, which are skewed with respect to the plane of velocity and velocity gradient.

A characteristic oscillating response in shear and normal stresses after a change of the shear rate is predicted for materials that are non-flow-aligning. Oscillations in shear stress, normal stress difference, or optical response have been found for lyotropic nematic solutions of poly(benzyl glutamate) (PBG),[13−19] hydroxypropylcellulose (HPC),[20,21] and other lyotropic LCPs,[22,23] as well as for thermotropic main-chain LCPs.[24−32] Low-molecular-weight nematics usually belong to the flow-aligning type, except when they have a smectic phase at lower temperature.[33] In the latter case, they are non-flow-aligning at temperatures not too high above the smectic−nematic phase transition, and oscillatory responses in the transient stresses have been found.[33−35] Regarding the sign of N_1, negative values have been reported for lyotropic LCPs,[3,36] but there is no clear evidence of negative N_1 in thermotropic LCPs.[37]

The flow properties of side-chain LCPs have been studied by only a few groups in the past years.[34,35,38−52] The first results led to apparently contradictory conclusions because both flow-aligning and non-flow-aligning behavior were found. Zentel and Wu[38] studied the steady-state viscosities of nematic side-chain LCPs with polysiloxane and polyacrylate backbones having smectic phases at lower temperatures. They found that the viscosity of the nematic phase is higher than that of the isotropic phase and concluded that the rheological behavior in side-chain LCPs is dominated by the flexible backbone and that flow does not induce a macroscopic orientation. A similar conclusion was reached by Colby et al.,[39] who found a similar linear viscoelastic behavior in the isotropic and nematic phases of polyacrylate side-chain LCPs under small-amplitude oscillatory shear. In contrast, Kannan et al.[40,41] and Rubin et al.[42] observed that the linear viscoelasticity of side-chain LCPs depends strongly on the molecular weight and that large-amplitude oscillatory shear produces a macroscopic orientation in nematic side-chain LCPs. Berghausen et al.[43] investigated the influence of shear on side-chain LCPs with laterally (side-on) fixed mesogenic groups. They could obtain well-aligned samples in creep experiments but not in oscillatory shear. As with Rubin et al.,[42] they also found that the rheological properties depend on the molecular weight. Non-flow-aligning behavior was also found by Jamieson and coworkers,[34,35,44−46] who studied the transient shear stress in monodomains of solutions of side-chain LCPs with oblate conformation in flow-aligning low-molecular-weight nematics.

The rheo-NMR technique developed in our lab provides simultaneously the director orientation under shear, via deuterium NMR spectroscopy, and the shear viscosity.[47] The determination of the Leslie coefficients and the shape of the spectra allow us to clearly differentiate between a flow-aligning or a non-flow-aligning nematic. Different side-chain LCPs have been investigated.[47−51] Our first results obtained by rheo-NMR made evident that side-chain LCPs can be either flow aligning[47] or non-flow-aligning.[48] More recent investigations[49−52] proved that the non-flow-aligning behavior of side-chain LCPs is related to the strength of smectic fluctuations in the nematic phase, similar to low-molecular-weight nematics. By changing temperature or composition (in the case of copolymers), it is possible to control the strength of these smectic fluctuations and to tune the flow behavior of side-chain LCPs.[49,50]

Scheme 1. Chemical Structure of the Side-Chain LCPs

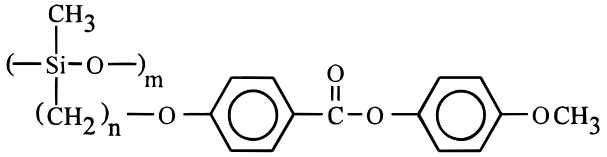

Apart from these studies, other aspects of the flow behavior of thermotropic side-chain LCP melts, like the shear stress (σ) and the first normal stress difference (N_1), remained to be investigated. In this contribution, we focus on the time-dependent response of σ and N_1 in shear-rate-controlled experiments for two side-chain LCPs with polysiloxane backbone that were previously studied by rheo-NMR.[47,49,50] Although there is only a small difference in chemical structure—the length of the spacer linking the mesogens to the backbone differs by two methylene units—the flow behavior of the polymers is completely different. The polymer with the shorter spacer, PSi4, is flow-aligning, whereas the other one, PSi6, is non-flow-aligning. The non-flow-aligning character of PSi6 has been related to its different phase behavior, showing a low-temperature smectic phase. Since the flow behavior of these polymers is already known, they can be considered as model systems for the present study of the transient stresses in various shear experiments. In particular, we investigate under which conditions a reproducible oscillatory response can be observed in the non-flow-aligning side-chain LCP. The stress transients of the non-flow-aligning system are analyzed in terms of Ericksen's transversely isotropic fluid model.[1,22,33−35,44−46]

2. Experimental Section

2.1. Materials. The two side-chain liquid crystalline polymers studied, presented in Scheme 1, consist of a polysiloxane backbone and a 4-methoxyphenyl-4′-alkyloxybenzoate side chain. The mesogen is connected to the backbone via a flexible spacer of four or six methylene units for PSi4 and PSi6, respectively. The synthesis was carried out as described by Finkelmann et al.[53] and Disch et al.[54] The degree of polymerization is about 80. Both polymers have a broad nematic phase, while only PSi6 shows also a smectic A phase. The transition temperatures determined by differential scanning calorimetry are 277 K for the glass transition (T_g) and 367 K for the nematic−isotropic transition (T_{ni}) of PSi4, and for PSi6, T_g = 271 K, T_{sn} = 311 K (smectic−nematic transition), and T_{ni} = 376 K.

2.2. Rheological Measurements. Rheological measurements were carried out with a Rheometrics RMS800 rheometer equipped with a transducer with a lower resolution limit of 2 g cm. Most experiments were performed in cone-and-plate geometry with a cone angle of 0.1 rad, a diameter of 25 mm, and a distance (gap) of 50 μm between the truncated cone and plate. Additional measurements were done using plate−plate geometry with a diameter of 25 mm and a gap of about 1 mm.

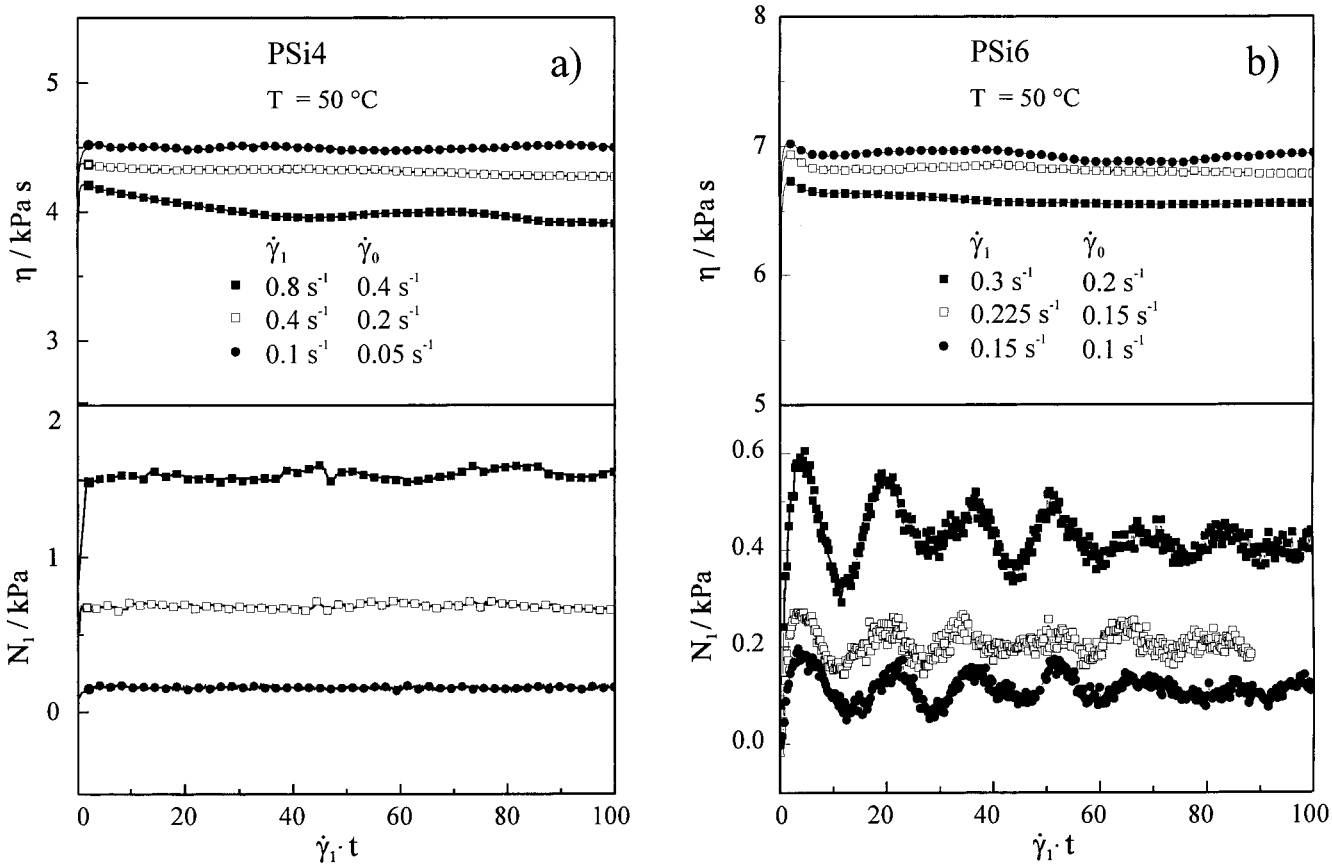

Figure 1. Transient response of viscosity (η) and first normal stress difference (N_1) vs the applied strain ($\dot{\gamma}_1 t$) after step increase of the shear rate for PSi4 (a) and PSi6 (b) at 50 °C at different shear rates $\dot{\gamma}_1$. The samples were presheared at $\dot{\gamma}_0$ and subsequently sheared at $\dot{\gamma}_1$.

Measurements of the transient stresses were carried out in the nematic phase. Both polymers were investigated in a broad range of temperatures in the nematic phase (50−90 °C). The shear rate was varied between 0.05 and 4 s^{-1}. For filling the shear cell the following procedure was used: the sample was placed into the gap in the isotropic state at 120 °C, then the gap was set and the sample was held at this temperature for 10 min, and finally the sample was cooled to the desired temperature. During cooling the gap was slowly adjusted to compensate for the thermal contraction of the metal. The first measurement was performed after a waiting time of 30 min to allow the sample to equilibrate. The shear history of the LCP samples has a strong effect on the rheological response. We used different kinds of experiments to study the time-dependent characteristics of the LCPs under flow. The kinematics of these experiments is described by denoting the different shear rates used in an experiment by $\dot{\gamma}_i$, where i = 0, 1, ..., n. In most of the experiments the sample was presheared at a rate $\dot{\gamma}_0$ and subsequently sheared at a rate $\dot{\gamma}_1$. Thus, for a start-up experiment $\dot{\gamma}_0 = 0$, and for a simple flow reversal experiment the sample is initially sheared at $\dot{\gamma}_0$ and then at $\dot{\gamma}_1 = -\dot{\gamma}_0$. Other shear histories were also applied, like stepwise increase or decrease of shear rate and preshear followed by squeezing or stretching of the sample between the cone-and-plate tools.

3. Results and Discussion

3.1. Comparison of PSi4 and PSi6. An example illustrating the different rheological behavior of the two polymers PSi4 and PSi6 is given in Figure 1, showing the transient values of the viscosity η and the first normal stress difference N_1 as a function of the applied strain $\gamma = \dot{\gamma}_1 t$ after stepwise increase of the shear rate at 50 °C. In Figure 1a, η and N_1 are presented for a PSi4 sample sheared at $\dot{\gamma}_1 = 0.8$, 0.4, and 0.1 s^{-1} after preshearing at $\dot{\gamma}_0 = 0.4$, 0.2, and 0.05 s^{-1}, respectively. There is no oscillatory behavior neither in η nor in N_1 for PSi4. Figure 1b shows η and N_1 for PSi6 sheared at $\dot{\gamma}_1 = 0.3$, 0.225, and 0.15 s^{-1} after preshearing at $\dot{\gamma}_0 =$ 0.2, 0.15, and 0.1 s^{-1}, respectively. PSi6 exhibits oscillations in N_1, but not in η under these experimental conditions. The oscillations scale quite well with the strain; however, their amplitude is rather small in the experiment shown.

The transients in Figure 1 show the characteristic difference between the two polymers. For PSi4 no oscillatory response was found, irrespective of temperature and shear rate. PSi6, on the other hand, exhibits oscillating transient stresses, in particular N_1, at all temperatures studied and in the whole range of shear rates applied. The intensity of the oscillations decreases with rising temperature so that for temperatures near the nematic−isotropic transition higher shear rates had to be applied in order to produce strong enough oscillations that could be analyzed quantitatively. The different rheological transients of PSi4 and PSi6 are in good agreement with the results from previous NMR experiments and confirm that PSi4 is a flow-aligning nematic,[47] whereas PSi6 is non-flow-aligning.[50] The oscillations of PSi6 become stronger at lower temperatures, closer to the nematic−smectic transition.

Further examples of stepwise change experiments on PSi6 are shown in Figures 2 and 3. In that case, a higher shear rate of $\dot{\gamma}_0 = 1.5$ s^{-1} was applied for the preshear, which leads to stronger oscillations. In parts a and b of Figure 2, the shear rate was decreased to $\dot{\gamma}_1 = 0.4$ s^{-1} after about 400 or 900 strain units, respectively. The

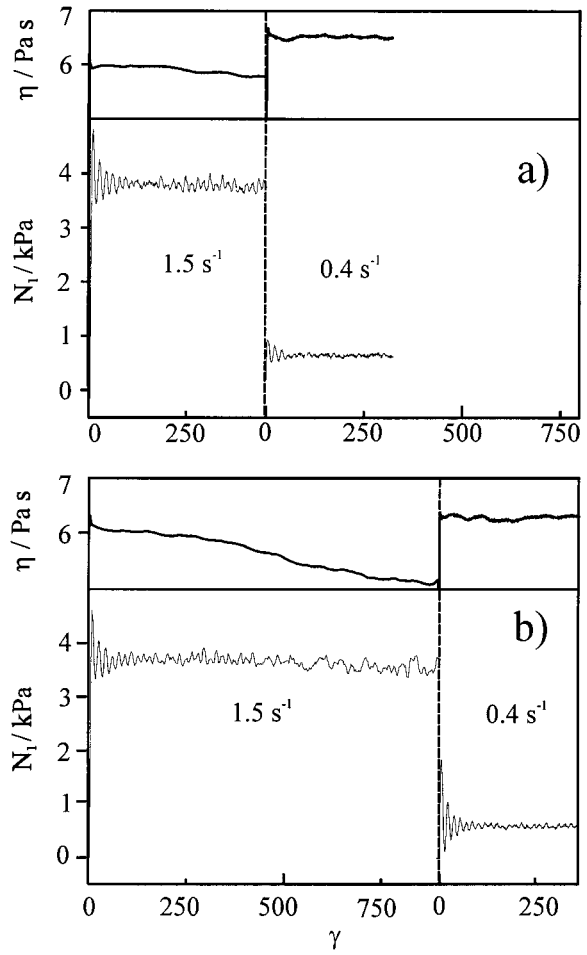

Figure 2. Viscosity (η) and first normal stress difference (N_1) vs the applied strain ($\gamma = \dot{\gamma}_0 t$ or $\gamma = \dot{\gamma}_1 t$) during preshear at $\dot{\gamma}_0$ and after step decrease of the shear rate to $\dot{\gamma}_1$ for PSi6. The oscillations are stronger after longer duration of the preshear.

comparison shows that a longer preshearing period leads to stronger oscillations. In addition, a significant decrease of the viscosity is noticed when the preshear is applied long enough. The experiment was repeated for different values of $\dot{\gamma}_1$, and the results are shown in Figure 3. The stress transients exhibit a scaling in strain and intensity; that is, a plot of the stress normalized to its steady-state value as a function of strain, as shown in Figure 3, yields a curve that is independent of the shear rate.

The stepwise change experiments of Figures 1−3 show that the amplitude of the oscillations depends on the mechanical history of the sample. In addition, the shape of the transients is also influenced by experimental details. Before exploring this in more detail, we will consider the steady-state behavior of the two polymers.

3.2. Steady-State Values of η and N_1. Parts a and b of Figure 4 show doubly logarithmic plots of the steady-state values of η and N_1, respectively, vs shear rate for PSi4 and PSi6. Both polymers show a slight shear thinning, although the viscosity is almost independent of the shear rate. Comparing this result with the three regions according to Onogi and Asada,[7] we characterize the observed behavior as region II (Newtonian) behavior. For the limited range of shear rates studied, there is no clear evidence of other regions, except for an indication of a decrease in η at higher shear rates for PSi6 at 50 °C. In fact, the last three data points shown on this curve are not the steady-state

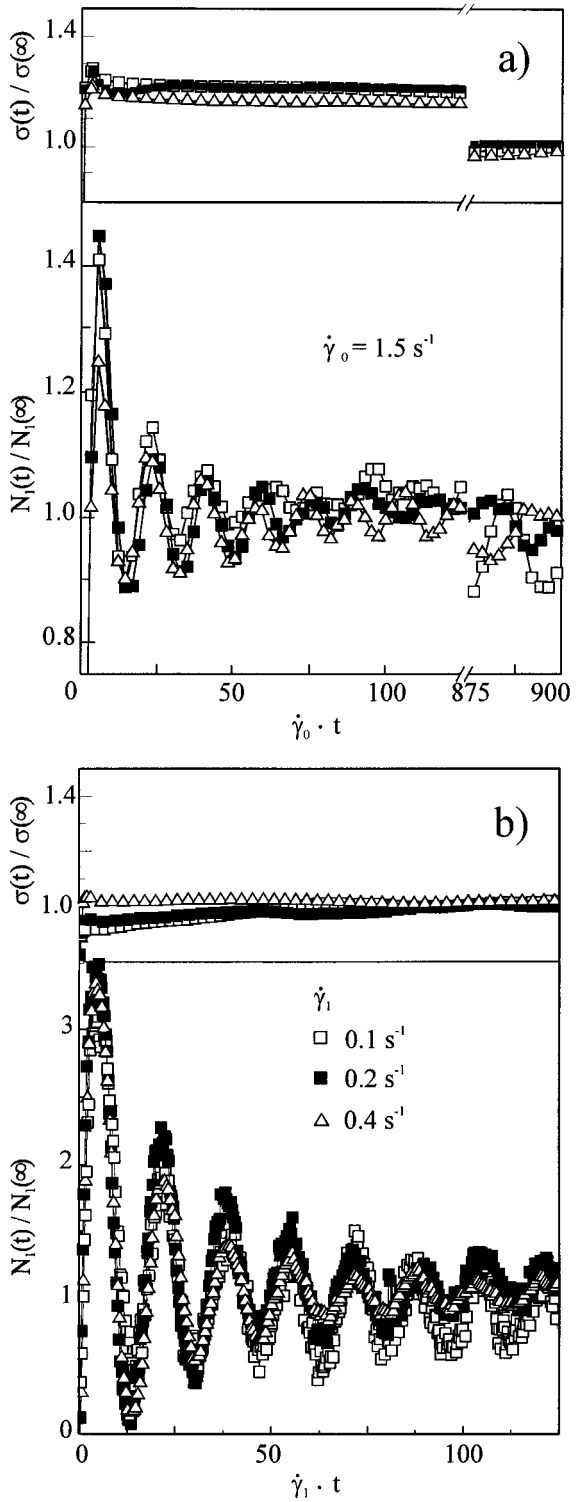

Figure 3. Reduced shear stress ($\sigma(t)/\sigma(\infty)$) and reduced first normal stress difference ($N_1(t)/N_1(\infty)$) for the step decrease experiment of Figure 2b and additional experiments with different $\dot{\gamma}_1$ before (a) and after (b) the step in shear rate from $\dot{\gamma}_0$ to $\dot{\gamma}_1$.

values as the viscosity was still decreasing when the experiments were stopped. Thus, there might exist a region III with shear thinning at higher shear rates.

The steady-state values of N_1 are always positive, and they increase with increasing shear rate, following the power law $N_1 = A\dot{\gamma}^m$, as shown in Figure 4b. The exponent m is 1.5 for PSi6 at 50 °C, 1.3 for PSi6 at 60 °C, and 1.1 for PSi4 at 50 °C. The values of m close to

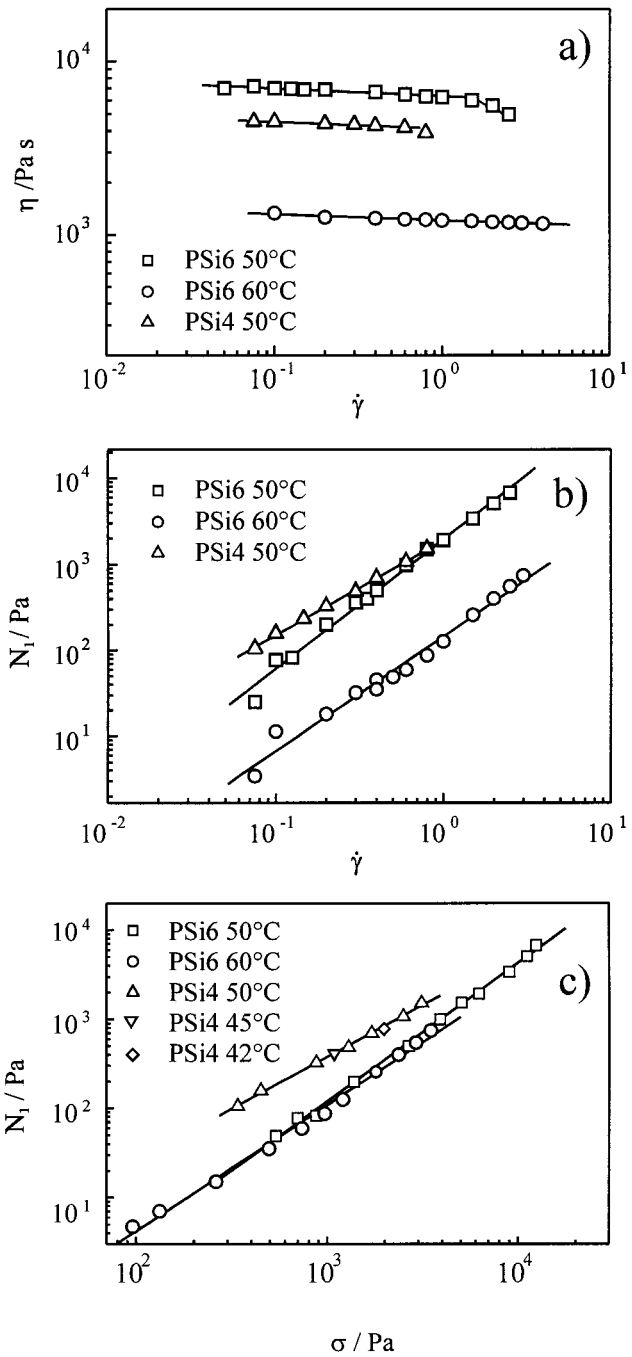

Figure 4. Steady-state values of η (a) and N_1 (b) as a function of shear rate $\dot{\gamma}$, and N_1 versus σ (c) for PSi4 (50 °C) and PSi6 (50 and 60 °C).

1 are similar to the values reported in the literature for other LCPs[23,31] but fall also within the range observed for non-liquid-crystalline polymers, for which m is typically in the range $1 < m \leq 2$. In the limited range of shear rates studied we do not find the behavior characteristic of lyotropic LCPs, for which N_1 increases with increasing shear rate up to a critical shear rate beyond which N_1 decreases and becomes negative.

Figure 4c shows that the first normal stress difference as a function of shear stress also follows approximately a power law, $N_1 = B\sigma^n$. The data for a given polymer at different temperatures fall on one master curve as expected. This holds for PSi6 with data points for two different temperatures as in Figure 4a,b and for PSi4, for which additional data points at 42 and 45 °C are plotted. The slope of the curve for PSi6 yields $n = 1.5$ and 1.4 at 50 and 60 °C, respectively, whereas $n = 1.2$ for PSi4. The values of N_1 at a given shear stress are higher for PSi4 than for PSi6, indicating that PSi4 with its shorter side chains is more elastic. We note that the N_1 vs σ curve of a random copolymer containing a mixture of 4- and 6-unit spacers (PSi4+6)[51] falls between those of PSi4 and PSi6, indicating an intermediate elasticity. Whether the observed differences of the steady-state stresses are a consequence of the different flow behavior or whether they are related to the different structure of the side-chain polymers remains to be further investigated.

3.3. Effect of the Mechanical History. *Flow Start-Up.* In contrast to stepwise change experiments, which sometimes yield only weak oscillations in N_1 (cf. Figure 1) and no oscillations in η (cf. Figures 1−3), start-up experiments generally result in transients with strong oscillations, observable for both shear and normal stresses.

Since a quantitative analysis of oscillating transients can be best performed if the oscillation amplitude is large, we investigated whether reproducible transients can be obtained in start-up experiments. After adjusting temperature and gap, the samples were allowed to relax for 30 min prior to shearing. As an example, Figure 5 shows transients of η and N_1 for a PSi6 sample at 50 °C for several values of $\dot{\gamma}_1$ (in start-up experiments $\dot{\gamma}_0 = 0\ s^{-1}$). The transients of η are reasonably reproducible. They always start with the same phase and scale with the strain, suggesting that start-up experiments can be used for an analysis of the oscillations. However, the N_1 transients for different shear rates exhibit no clear pattern. The oscillations start with different, apparently random phases; only their period is similar. Thus, a scaling in strain and intensity is not possible for N_1. The N_1 transients, in particular, demonstrate how crucially the rheological response depends on the initial conditions, a fact well-known from other liquid crystal polymers.

The observed differences in the transient N_1 curves can be attributed to the squeezing and stretching processes that occur during the setting of the gap and the temperature. Achieving a reproducible initial structure in start-up experiments is difficult because, on one hand, it is necessary to squeeze the sample in order to set the gap, but on the other hand, the sample is stretched between the tools because of their contraction with decreasing temperature. Since mechanical stresses during the preparation of the sample cannot be avoided in start-up experiments, the initial state is ill-defined. Therefore, start-up experiments are not suitable for a quantitative analysis of the transients. Stepwise change experiments, on the other hand, though yielding better controlled initial states, often result in weak oscillations for our samples. Therefore, we sought another procedure, which imposes a well-defined mechanical history on the sample while at the same time generating strong oscillations from which further information can be extracted.

Squeezing and Stretching. As implied by the start-up experiments, squeezing or stretching of the sample between the tools has a strong effect on the stress transients. To analyze this effect, a sample in the cone-and-plate cell was subjected to controlled squeezing or stretching after a period of preshear. These experiments were performed as follows: The sample was presheared

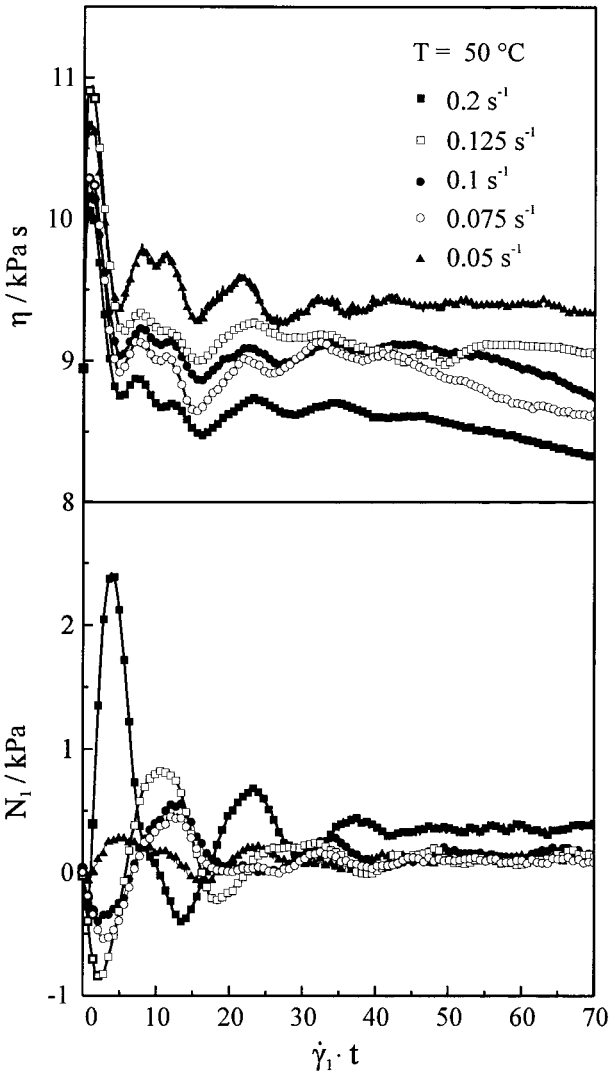

Figure 5. Transient response of η (top) and N_1 (bottom) vs $\dot{\gamma}_1 t$ in flow start-up experiments on PSi6 at a temperature of 50 °C at different shear rates $\dot{\gamma}_1$ as given in the figure.

at $\dot{\gamma}_0$ with a gap of 50 μm $\pm$ d_s, until the steady state was reached, then the gap was changed to 50 μm, and the sample was sheared at $\dot{\gamma}_1$. The degree of squeezing or stretching, d_s, has a value of a few micrometers up to several tens of micrometers. In both cases, after squeezing or stretching, very intense oscillations are observed. Figure 6 shows the transient response of η and N_1 vs $\dot{\gamma}_1 t$ ($\dot{\gamma}_1 = 0.2$ s^{-1}) after squeezing (dotted line) and after stretching (solid line) by approximately 15 μm of the presheared sample ($\dot{\gamma}_0 = 0.2$ s^{-1}) at a temperature of 50 °C. Both squeezing and stretching have a strong effect on the alignment of the director in the sample. In both cases the director is turned away from the steady-state orientation adopted during preshearing. The initial state of orientation generated by squeezing or stretching thus is different from the steady state, and the subsequent rotations of the director when shear is started again give rise to the strong oscillations.

Squeezing and stretching yield similar transient viscosities, but a different response in N_1; cf. Figure 6. When the sample is stretched, the first oscillation of N_1 is positive. On the other hand, when the sample is squeezed, the first oscillation of N_1 is negative. The oscillations are damped but can be followed for 15 cycles or more. The oscillations persist much longer than in the case of main-chain thermotropic or lyotropic LCPs,

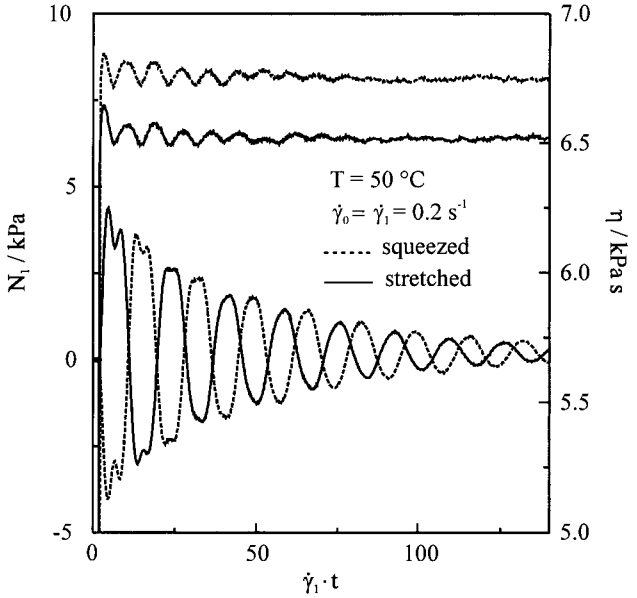

Figure 6. Effect of squeezing and stretching on the transient behavior of η (curves at top) and N_1 (curves at bottom) for two samples of PSi6 at 50 °C. Both samples were presheared at $\dot{\gamma}_0 = 0.2$ s^{-1}, and then one was squeezed and the other one stretched before they were sheared again at $\dot{\gamma}_1 = 0.2$ s^{-1}.

where the oscillations typically disappear after four or five cycles. In this respect, the oscillatory pattern of the non-flow-aligning side-chain LCP investigated here resembles that of low-molecular-weight nematics[33] rather than that of other types of LCPs. The differences, however, may be merely a consequence of the state of director orientation in the sample. Experiments on low-molecular-weight nematics are typically performed on monodomain samples, whereas polydomain samples have been used in most experiments on bulk LCPs.

The different sign of the first oscillation of N_1 is obviously related to a different orientation of the director, since squeezing and stretching lead to different orientations. This aspect will be further discussed below. The amplitude of the oscillations appears to be related to the degree of the alignment: the more uniform the orientation, the stronger the oscillations. This is illustrated by an experiment in which the degree of squeezing is varied. Figure 7a shows several transients of N_1 for increasing d_s, and Figure 7b shows the dependence of the oscillation amplitude on d_s. For this experiment, the sample was cooled from the isotropic state to 50 °C, and the gap was set to 50 μm + d_s. With this gap the sample was presheared at $\dot{\gamma}_0 = 0.2$ s^{-1} for a period of 1500 s, then the gap was reduced to 50 μm, and the sample was sheared again at $\dot{\gamma}_1 = 0.2$ s^{-1}. The transients in Figure 7a illustrate how the amplitude of the oscillations grows with increasing d_s, while at the same time double peaks develop. In Figure 7b, the magnitude of N_1 at the first minimum ($N_{1\max}$) is presented vs d_s. Similar effects were observed in the transient viscosity. This experiment shows that the better orientation achieved by a higher degree of squeezing leads to stronger oscillations. In additional experiments we found that there is an optimum for the degree of squeezing. Squeezing the sample too much leads to a deterioration of the alignment and to a corresponding decrease in the amplitude of the oscillations.

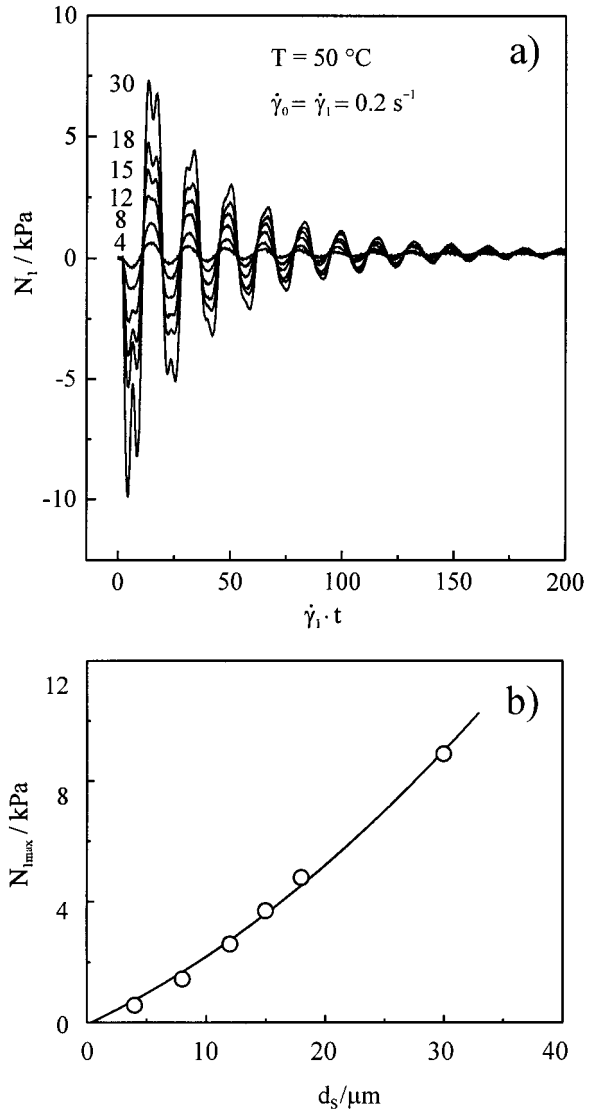

Figure 7. Effect of the degree of squeezing d_s on the transient behavior of N_1 for PSi6 at 50 °C. The samples were presheared at $\dot{\gamma}_0 = 0.2\ s^{-1}$, then squeezed, and sheared again at $\dot{\gamma}_1 = 0.2\ s^{-1}$. (a) N_1 as a function of strain $\dot{\gamma}_1 t$, with d_s given in μm; (b) magnitude of the first minimum of the curves in (a) as a function of the degree of squeezing d_s.

The role of the preshearing period in a stretching experiment was investigated in plate−plate geometry. In this case, the difference $N_1 - N_2$ is obtained, where N_2 is the second normal stress difference. The shear rate is not constant in this geometry; the values quoted refer to the maximum shear rate at the edge of the cell. The sample was filled in at 120 °C, the gap was set at this temperature, and then the sample was cooled to 50 °C, with the tools kept in constant positions. Thermal contraction results in a well-defined stretching of the sample. One experiment was performed without preshear ($\dot{\gamma}_0 = 0\ s^{-1}$) and another one after a preshear at $\dot{\gamma}_0 = 0.05\ s^{-1}$. The results are shown in Figure 8. Without preshear the damping is much stronger than after preshear, indicating that preshear plus stretching yields a better alignment than simple stretching. The presheared sample behaves more like a monodomain, whereas without preshear the sample is more like a polydomain with only a minor orientational bias due to the stretching. Thus, the combination of preshear and stretching or squeezing seems to be an efficient method to generate a well-defined initial

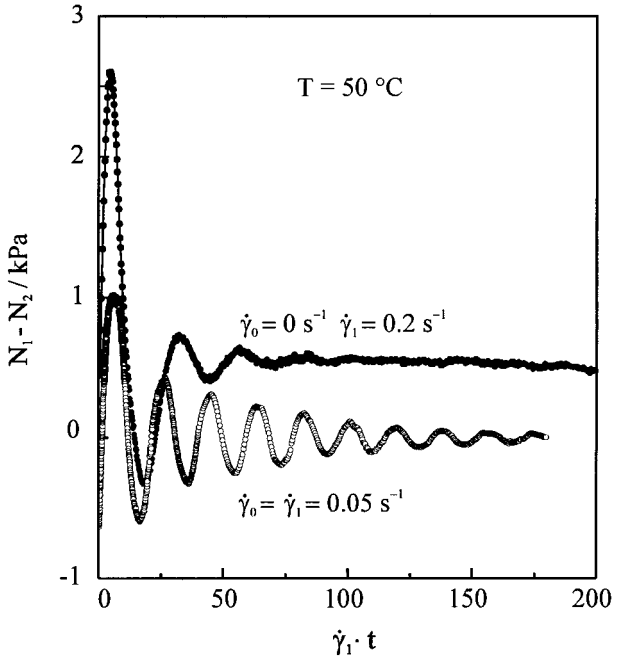

Figure 8. Transient response of $N_1 - N_2$ vs $\dot{\gamma}_1 t$ after stretching an unpresheared sample (●) and a presheared sample (○) in plate−plate geometry. The stretching of the sample was achieved by filling the tools with the isotropic sample at a temperature of 120 °C and then cooling to 50 °C while the tools were kept in fixed position so that the sample was stretched by the metal contraction.

state. An indication that the state of the sample after such a treatment is indeed well-defined is the fact that the transient stresses can be scaled by their steady-state values.

In Figure 9a the reduced first normal stress difference $N_1(t)/N_1(\infty)$ and the reduced shear stress $\sigma(t)/\sigma(\infty)$ are presented as a function of $\gamma = \dot{\gamma}_1 t$ for PSi6 sheared at $\dot{\gamma}_1 = 0.2\ s^{-1}$ after preshearing at the same shear rate ($\dot{\gamma}_0 = 0.2\ s^{-1}$) and squeezing by $d_s = 30\ \mu$m. Figure 9b depicts the reduced normal stress difference vs the reduced shear stress. This type of graph was suggested by Maffettone et al.[55] as a fingerprint of the material response. The transient stresses of PSi6, shown in Figure 9, do not look like any other reported in the literature. The oscillations are much more intense in N_1, about 40 times larger than in the shear stress. In addition to the oscillations, there is a decrease of the shear stress until the steady state is eventually reached. Furthermore, PSi6 exhibits the interesting phenomenon that σ and N_1 have different strain periods. The frequency of the shear stress is twice as large as that of the first normal stress difference. This behavior, which is discussed in section 3.4, has been reported recently also for side-chain LCPs with slightly different mesogens, but no explanation can be given.[51]

Flow Reversal. An example of a flow reversal experiment is shown in Figure 10. PSi6 was presheared at $\dot{\gamma}_0 = 0.1\ s^{-1}$ until the steady state was reached, squeezed in order to generate intense oscillations, and sheared again at $\dot{\gamma}_1 = 0.1\ s^{-1}$. The direction of the flow was changed for a first time ($\dot{\gamma}_2 = -\dot{\gamma}_1$) after four cycles of N_1. In this case the oscillations are refocused; that is, their damping is reversed until a maximum is reached after a time interval identical to the duration of shear before the flow reversal. When the flow is reversed, a

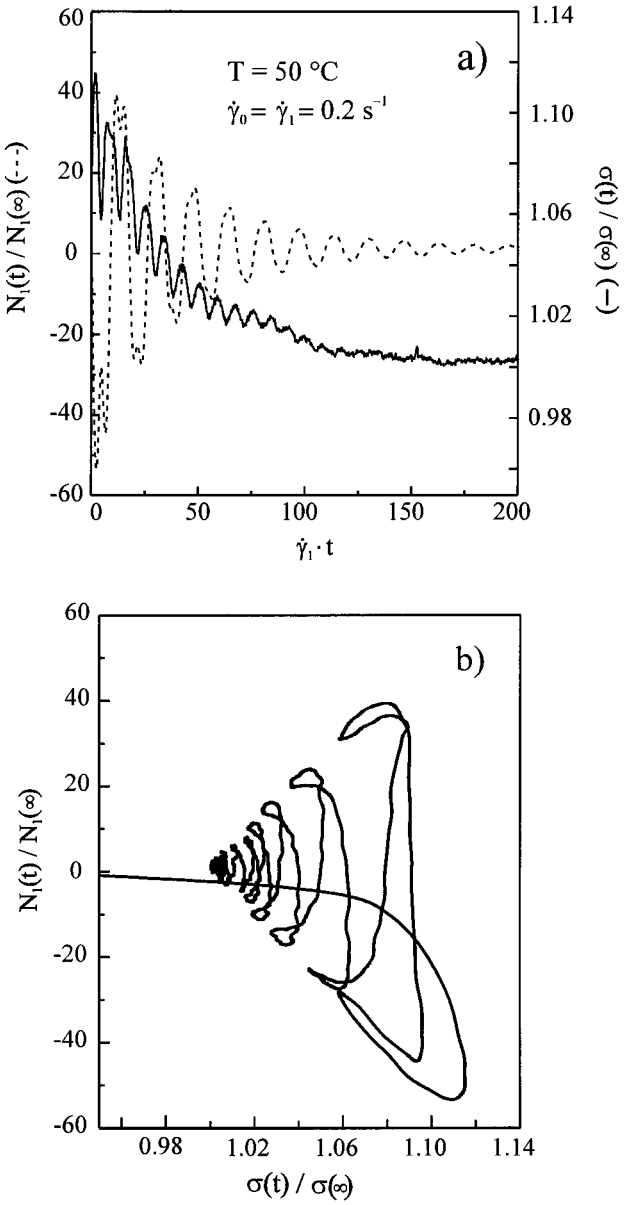

Figure 9. (a) Reduced N_1 (dashed line) and reduced σ (solid line) vs $\dot\gamma_1 t$ at $\dot\gamma_1 = 0.2\ s^{-1}$ and 50 °C, in a sample of PSi6 presheared at $\dot\gamma_0 = 0.2\ s^{-1}$ and squeezed by 30 μm. (b) Reduced N_1 vs reduced σ for the data shown in (a).

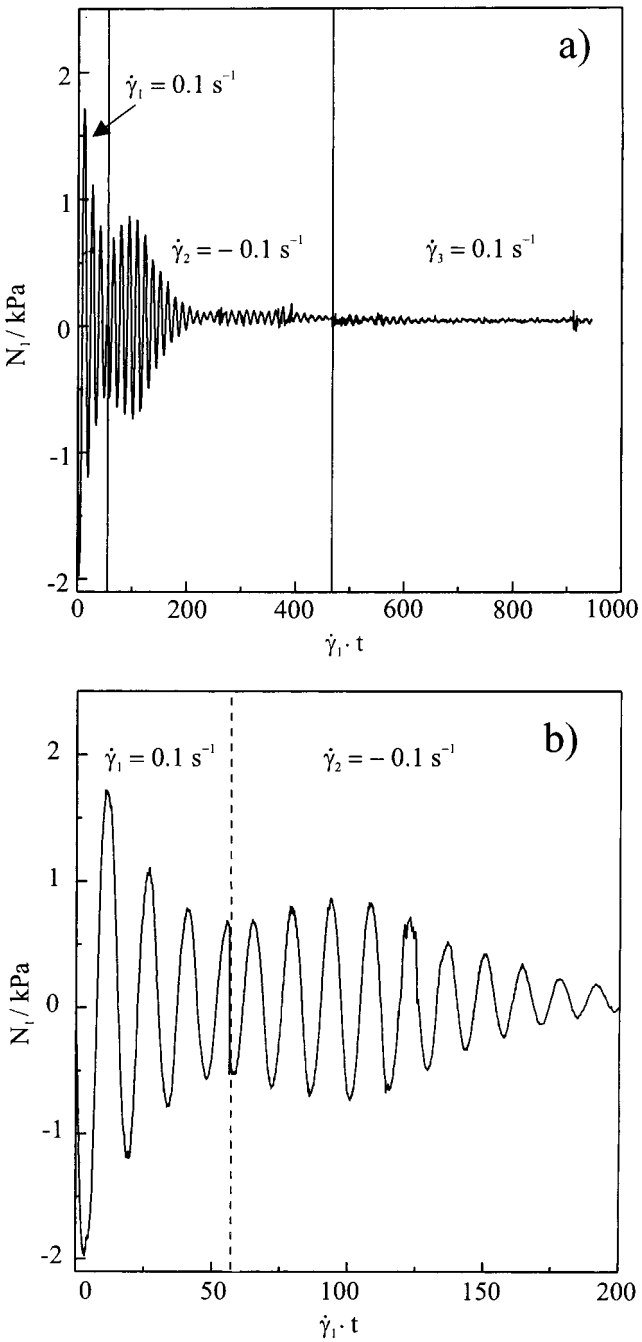

Figure 10. Transient N_1 response in a flow reversal experiment on PSi6 at an absolute shear rate of 0.1 s^{-1} at 50 °C in a sample previously sheared and squeezed. The switching of the flow direction occurs twice, at strains of ca. 50 and 460 strain units. (b) A blow-up of (a).

phase shift is observed in the N_1 oscillations. This phase shift results from the reversal of the velocity direction, which corresponds to a sudden change of the director orientation relative to the velocity axis. In other similar experiments we observed that the maximum intensity of the refocused oscillations is always smaller than the initial maximum. In the experiment shown in Figure 10, the flow direction was changed for a second time ($\dot\gamma_3 = -\dot\gamma_2 = \dot\gamma_1$) after N_1 had reached its steady-state value. In this case, the oscillations are not refocused and do not reappear. For comparison, Figure 11 shows the behavior of the flow-aligning system PSi4 upon flow reversal. There is always an undershoot in N_1 after the flow is reversed.

The behavior of PSi6 is different from other non-flow-aligning systems such as PBG or HPC. For those systems new oscillations always occur after a switching of the shear direction, even after an extended duration of the first interval of shearing. Therefore, flow reversal can be used to generate oscillations, and no squeezing or stretching is required. The phenomenon of refocused oscillations has not been observed in PBG or HPC. Refocusing, however, was found for monodomains of low-molecular-weight nematics[33] and of solutions of side-chain LCPs in a low-molecular-weight nematic.[34,35]

The recurrence of oscillations upon flow reversal may depend on whether the orientational distribution of the director at the time of flow reversal still has a nonzero component in the velocity−velocity gradient plane. If the director is completely aligned along the vorticity axis (log-rolling), its orientation is invariant to flow reversal; hence, no reappearance of oscillations is expected. Thus, the absence of oscillations after flow reversal at higher

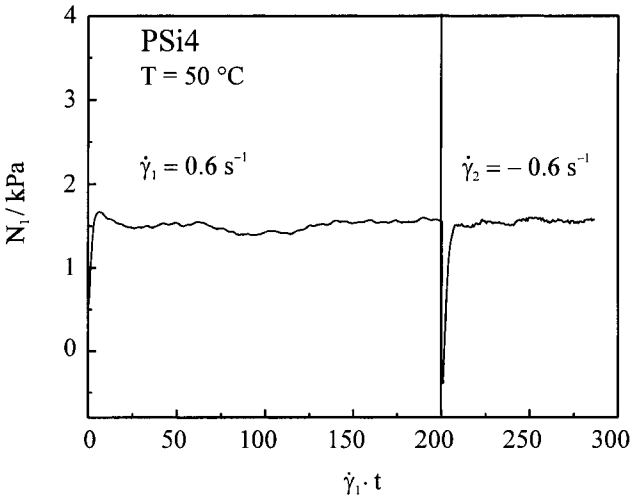

Figure 11. Transient N_1 response in a flow reversal experiment on PSi4 at an absolute shear rate of 0.6 s^{-1} at 50 °C. An undershoot is observed.

strains in PSi6 can be taken as evidence for the log-rolling orientation of the director. This orientation of the director parallel to the vorticity axis has already been observed in PSi6 by Siebert in neutron scattering experiments.[50] When applying oscillatory shear to a nematic end-on side-chain polymethacrylate with a spacer of six methylene groups, Kannan et al.[40] also found that the mesogenic groups were oriented perpendicular to the flow direction, parallel to the vorticity axis. Larson and Öttinger predict for the log-rolling case that the approach to the vorticity axis is very slow, slower than the approach to the velocity−velocity gradient plane, when this plane is the attractor, as in the case of tumbling.[12] This slow approach to the steady state of log-rolling may explain why the oscillations of the non-flow-aligning system investigated here persist up to rather high strains.

3.4. Analysis of the Stress Transients of the Tumbling LCP. The shape of the stress transients can be modeled by using Ericksen's transversely isotropic fluid model.[1,22,33−35,44−46] The director is assumed to be confined in the deformation plane spanned by the velocity and the velocity gradient. The director orientation with respect to the velocity gradient axis is given by θ. For a tumbling nematic θ depends on the strain γ according to

$$\tan\theta = \left(\frac{-\alpha_2}{\alpha_3}\right)^{0.5} \tan\left(\frac{(-\alpha_2\alpha_3)^{0.5}}{\alpha_3 - \alpha_2}\gamma\right) \qquad (1)$$

The orientation dependence of the viscosity and normal stress difference is described by

$$\eta = \left[\alpha_1 + \frac{(\alpha_3 + \alpha_2)^2}{\alpha_3 - \alpha_2}\right]\sin^2\theta\cos^2\theta + \eta_b - \frac{{\alpha_3}^2}{\alpha_3 - \alpha_2} \qquad (2)$$

and

$$\frac{N_1}{\dot{\gamma}} = \left[\alpha_1 + \frac{(\alpha_3 + \alpha_2)^2}{\alpha_3 - \alpha_2}\right]0.5\sin 2\theta\cos 2\theta \qquad (3)$$

Here, α_1, α_2, and α_3 are Leslie coefficients, and $\eta_b = (\alpha_3 + \alpha_4 + \alpha_6)/2$ is the Miesowicz viscosity for the director parallel to the velocity. The strain period Γ corresponding to a director rotation by 2π is related to the reactive parameter λ by

$$|\lambda| = \sqrt{1 - \left(\frac{4\pi}{\Gamma}\right)^2} \qquad (4)$$

Since the viscosity transients observed for PSi6 are quite similar to those of monodomain nematics,[33−35,44−46] we modeled our data assuming a uniform director orientation in the deformation plane, although the initial state of the director orientation generated by preshear followed by squeezing is not known. We performed a fit to the viscosity data and used the resulting values of the fit parameters in a simulation of the N_1 transients. Before fitting we subtracted the exponential decay from the experimental viscosities. In the fitting function, we introduced an additional factor $1 - \exp(-p_2/\gamma)$ to describe the damping of the oscillations. To take into account the unknown initial orientation of the director after squeezing and strain delays resulting from mechanical inertia, γ in eq 2 was replaced by $\gamma + \gamma_0$. Thus, we obtain the following equation for fitting the viscosities:

$$\eta = p_1\left[1 - \exp\left(\frac{-p_2}{\gamma}\right)\right]\sin^2\left[\arctan\left[\frac{1}{p_3}\tan\left[\left(\frac{p_3}{{p_3}^2 - 1}\right)\times(\gamma + p_4)\right]\right]\right]\cos^2\left[\arctan\left[\frac{1}{p_3}\tan\left[\left(\frac{p_3}{{p_3}^2 - 1}\right)(\gamma + p_4)\right]\right]\right] + p_5 \qquad (5)$$

For the fit, $p_1 = \alpha_1 + (\alpha_3 + \alpha_2)^2/(\alpha_3 - \alpha_2)$, the damping constant p_2, $p_3 = \delta = (-\alpha_3/\alpha_2)^{1/2}$, and $p_4 = \gamma_0$ were used as free parameters, whereas $p_5 = \eta_b - {\alpha_3}^2/(\alpha_3 - \alpha_2)$ was set to the steady-state viscosity and kept fixed. The values of the parameters p_1, p_2, p_3, and p_4 obtained by fitting the viscosity were then used to simulate N_1.

The experimental and calculated transients are shown in Figures 12 and 13 for PSi6 at 50 and 60 °C, respectively. The strain period Γ shown in the plots corresponds to a director rotation by 2π. The agreement between experiment and model is fairly good for the viscosity curves, considering the fact that the assumption of a monodomain structure is rather crude. The more complicated orientational state of the sample is probably the reason for the poor resolution of the double peak structure of the viscosity. Experimental and simulated N_1 transients, on the other hand, show no agreement. First, the experimental N_1 curve exhibits a period twice as large as calculated for the model. According to eqs 2 and 3, the strain period should be the same for both η and N_1 and reflect the fact that a nematic system is invariant under a director rotation by π. This discrepancy was pointed out in a previous paper.[51] Second, in addition to the period, also the amplitude of the normal stress oscillations does not agree with the theoretical prediction. The experimental amplitude is about 2 orders of magnitude higher than the calculated one. To exclude any experimental error, the measurements were repeated on a different rheometer (Paar Physica UDS200). These experiments yielded the same results.

Fitting the data using eq 5 with p_4 as a free parameter leaves two choices for p_3 since p_3 and $p_3' = 1/p_3$ result in curves of the same shape that are just shifted along the γ axis. Since the initial director orientation is unknown, we chose to keep p_4 as free parameter and used the information from our previous NMR experi-

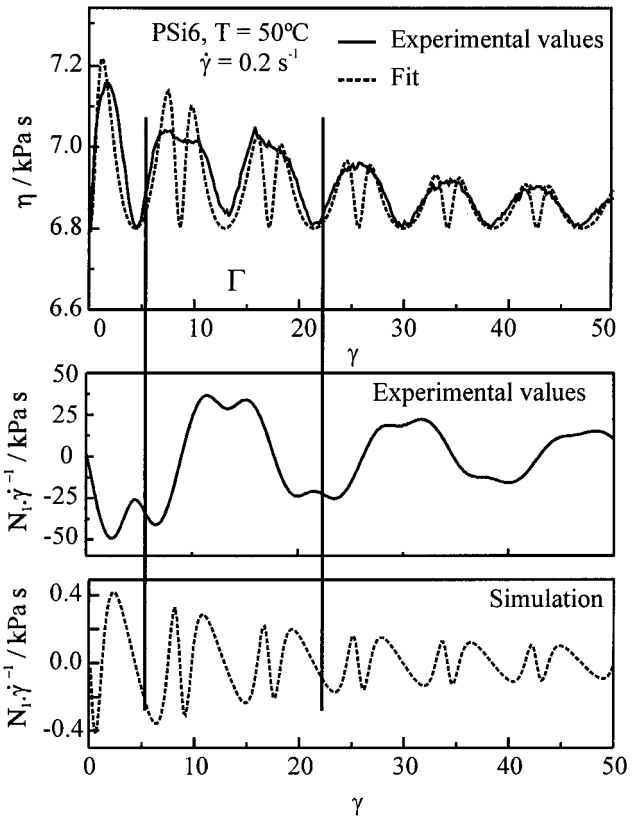

Figure 12. Fit of the viscosity (η) as a function of strain (γ) using eq 4 (top) and comparison of the experimentally observed first normal stress (N_1) (middle) with a simulation (bottom) using eq 3 and the parameters obtained by the viscosity fit for PSi6 at 50 °C. The vertical lines indicate one strain period.

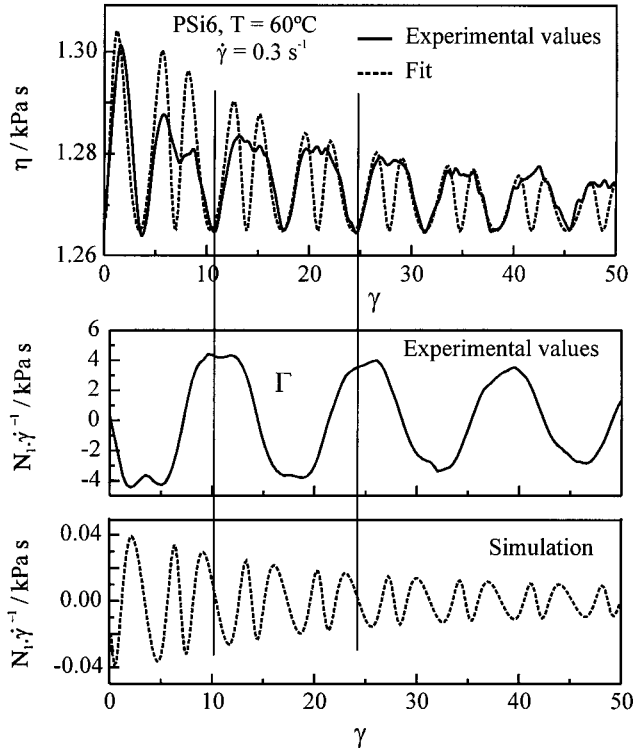

Figure 13. Fit of the viscosity (η) as a function of strain (γ) using eq 4 (top) and comparison of the experimentally observed first normal stress (N_1) (middle) with a simulation (bottom) using eq 3 and the parameters obtained by the viscosity fit for PSi6 at 60 °C. The vertical lines indicate one strain period.

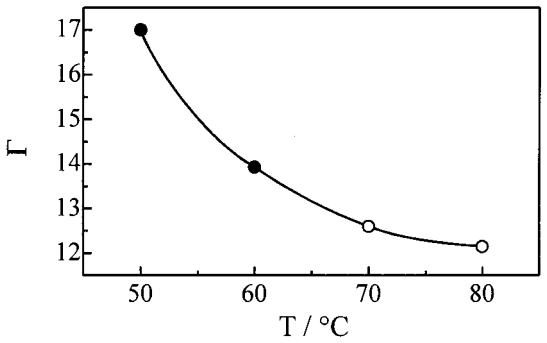

Figure 14. Temperature dependence of the strain period Γ of the N_1 oscillations. Filled symbols represent data obtained by fitting, and open symbols represent data obtained from a simple measurement of the strain period.

ments under shear that $|\alpha_3| > |\alpha_2|$.[50,51] From the resulting fit parameter p_3 and the rotational viscosity $\gamma_1 = \alpha_3 - \alpha_2$, the Leslie coefficients α_2 and α_3 have been calculated. We used γ_1 values obtained by a temperature interpolation of results from a deuteron NMR study of the director reorientation under shear in a magnetic field.[50] Assuming an anisotropy of the magnetic susceptibility of 10^{-6}, the NMR experiments yield $\gamma_1 = 8000$ Pa s at 50 °C and $\gamma_1 = 1050$ Pa s at 60 °C. Thus, for 50 °C α_2 and α_3 are −1300 and 6700 Pa s, respectively, and for 60 °C the values are −300 and 750 Pa s. Using α_2 and α_3, the Miesowicz viscosities η_b and $\eta_c = (-\alpha_2 + \alpha_4 + \alpha_5)/2 = \eta_b - \alpha_2 - \alpha_3$ can be calculated from p_5. We obtain $\eta_b = 12\,400$ Pa s, $\eta_c = 7000$ Pa s at 50 °C and $\eta_b = 1800$ Pa s, $\eta_c = 1350$ Pa s at 60 °C. A determination of α_1 from p_1 is not meaningful since the amplitude of the oscillations given by p_1 depends on the initial orientational distribution of the director and thus on experimental conditions such as the degree of squeezing. For our choice of p_3 based on the previous NMR experiments, the fit yields $\gamma_0 = 4.1$ and 3.5 at 50 and 60 °C, respectively. With strain periods of 17.01 and 13.93 at 50 and 60 °C, this corresponds to an initial director orientation θ_0 of approximately $\pi/2$; that is, the projection of the director on the velocity−velocity gradient plane is close to the velocity axis.

As mentioned above, the stress transients after squeezing and stretching (cf. Figure 6) start with the same phase in the case of η but differ in the sign of the first oscillation in the case of N_1. According to our analysis of the viscosity transients, this corresponds to a phase difference of the initial director component in the velocity−velocity gradient plane by π. This is surprising as one might have expected that squeezing and stretching lead to orientations differing by $\pi/2$.

For temperatures higher than 60 °C only the strain period Γ was determined from the N_1 transients. The temperature dependence of Γ is shown in Figure 14. The period decreases with increasing temperatures and levels off toward 4π, its minimum value according to eq 4, at high temperatures. From the period alone only the absolute values of the reactive parameter, $|\lambda|$, can be obtained according to eq 4, but our previous NMR experiments have shown that λ is negative.[50,51] The negative values of λ indicate that PSi6 has an oblate shape. Therefore, the Miesowicz viscosity for a director orientation parallel to the velocity gradient axis (η_c) is lower than the one for the director pointing along the velocity axis (η_b). The shape becomes the more anisotropic the lower the temperature, as the nematic−smectic phase transition is approached.

4. Conclusions

The stress transients observed for PSi4 and PSi6 confirm the flow-aligning behavior of PSi4 and the non-flow-aligning behavior of PSi6 found previously by NMR experiments. Furthermore, the reactive parameters of PSi6 determined by transient rheology and by rheo-NMR are in good agreement. Positive steady-state values of N_1, which increase with increasing shear rate, were found in both PSi4 and PSi6. In the investigated range of shear rates between 0.05 and 4 s^{-1} the viscosity depends only weakly on the shear rate, indicating region II behavior according to the classification by Onogi and Asada.

The tumbling behavior of PSi6 with its strong, weakly damped oscillations, which can be refocused by flow reversal, is more similar to low-molecular-weight systems than to liquid crystal polymers such as PBG and HPC. This could be a consequence of the relatively weak coupling between mesogens and polymer backbone in the side-chain LCPs. The polymer has the effect of increasing the viscosity, but the nematic flow behavior remains similar to that of small mesogenic molecules. The transient behavior of the shear stress can be described by the Ericksen model, but the deviation of the normal stress transients from this model remains to be explained.

The initial phase and the amplitude of the oscillations are related to the initial state of director orientation, which depends on the mechanical history of the sample. Squeezing or stretching after preshear has proven a useful technique for the generation of a controlled initial state that yields strong reproducible oscillations. The response to flow reversal is refocused oscillations, but only if the flow reversal is imposed while the preceding oscillations are still visible. The fact that no oscillations appear after flow reversal at higher strains can be explained by the log-rolling orientation of the director in the steady state.

Acknowledgment. This work was funded by the European Commission within its TMR program under Contract ERB-FMRX-CT96-0003, by the Deutsche Forschungsgemeinschaft, and by the Fonds der Chemischen Industrie.

References and Notes

(1) Larson, R. *The Structure and Rheology of Complex Fluids;* Oxford University Press: New York, 1999.
(2) Marrucci, G.; Greco, F. *Adv. Chem. Phys.* **1993,** *86*, 331−404.
(3) Moldenaers, P. In *Rheology and Processing of Liquid Crystal Polymers*; Acierno, A., Collyer, A., Eds.; Chapman & Hall: London, 1996; Chapter 8, pp 251−287.
(4) Burghardt, W. R. *Macromol. Chem. Phys.* **1998,** *199*, 471−488.
(5) de Gennes, P. G.; Prost, J. *The Physics of Liquid Crystals*, 2nd ed.; Oxford University Press: New York, 1993.
(6) Larson, R. G.; Doi, M. *J. Rheol.* **1991**, *35*, 539−563.
(7) Onogi, S.; Asada, T. In *Rheology*; Astarita, G., Marrucci, G., Nicolais, L., Eds.; Plenum Press: New York, 1980; Vol. 1, pp 127−147.
(8) Wissbrun, K. F. *J. Rheol.* **1981,** *25*, 619−662.
(9) Doi, M. J. *Polym. Sci., Polym. Phys. Phys. Ed.* **1981**, *19*, 229−243.
(10) Marrucci, G.; Maffetone, P. L. *Macromolecules* **1989**, *22*, 4076−4082.
(11) Larson, R. G. *Macromolecules* **1990**, *23*, 3983−3992.
(12) Larson, R. G.; Öttinger, H. C. *Macromolecules* **1991**, *24*, 6270−6282.
(13) Mewis, J.; Moldenaers, P. *Mol. Cryst. Liq. Cryst.* **1987**, *153*, 291−300.
(14) Berry, G. C.; Srinivasarao, M. *J. Stat. Phys.* **1991**, *62*, 1041−1059.
(15) Moldenaers, P.; Yanase, H.; Mewis, J. *J. Rheol.* **1991**, *35*, 1681−1699.
(16) Burghardt, W. R.; Fuller, G. G. *Macromolecules* **1991**, *24*, 2546−2555.
(17) Hongladarom, K.; Burghardt, W. R. *Macromolecules* **1993**, *26*, 785−794.
(18) Müller, J. A.; Stein, R. S.; Winter, H. H. *Rheol. Acta* **1996,** *35*, 160−167.
(19) Mewis, J.; Mortier, M.; Vermant, J.; Moldenaers, P. *Macromolecules* **1997**, *30*, 1323−1328.
(20) Grizzuti, N.; Cavella, S.; Cicarelli, P. *J. Rheol.* **1990**, *34*, 1293−1310.
(21) Metzner, A. B.; Prilutski, G. M. *J. Rheol.* **1986**, *30*, 661−691.
(22) Yang, I. K.; Shine, A. D. *Macromolecules* **1993,** *26*, 1529−1536.
(23) Mortier, M.; Moldenaers, P.; Mewis, J. *Rheol. Acta* **1996**, *35*, 57−68.
(24) Viola, G. G.; Baird, D. G. *J. Rheol.* **1986**, *30*, 601−628.
(25) Kalika, D. S.; Giles, D. W.; Denn, M. M. *J. Rheol.* **1990**, *34*, 139−154.
(26) Cocchini, F.; Nobile, M. R.; Acierno, D. *J. Rheol.* **1991**, *35*, 1171−1189.
(27) Guskey, S. M.; Winter, H. H. *J. Rheol.* **1991**, *35*, 1191−1207.
(28) Kim, S. S.; Han, C. D. *J. Rheol.* **1993**, *37*, 847−866.
(29) Han, C. D.; Kim, S. S. *J. Rheol.* **1994**, *38*, 13−30.
(30) Han, C. D.; Kim, S. S. *Macromolecules* **1993**, *26*, 6633−6642.
(31) Beekmans, F.; Gotsis, A. D.; Norder, B. *J. Rheol.* **1996**, *40*, 947−966.
(32) Beekmans, F.; Gotsis, A. D.; Norder, B. *Rheol. Acta* **1997**, *36*, 82−95.
(33) Gu, D.-F.; Jamieson, A. M. *J. Rheol.* **1994**, *38*, 555−571.
(34) Jamieson, A. M.; Gu, D.; Chen, F. L.; Smith, S. *Prog. Polym. Sci.* **1996**, *21*, 981−1033.
(35) Gu, D.-F.; Jamieson, A. M.; Wang, S. Q. *J. Rheol.* **1993**, *37*, 985−1001.
(36) Kiss, G.; Porter, R. S. *J. Polym. Sci., Polym. Symp.* **1978,** *65*, 193−211.
(37) Cocchini, F.; Nobile, M. R.; Acierno, D. *J. Rheol.* **1992,** *36*, 1307−1311.
(38) Zentel, R.; Wu, J. *Makromol. Chem.* **1986**, *187*, 1727−1736.
(39) Colby, R. H.; Gillmor, J. R.; Galli, G.; Laus, M.; Ober, C. K.; Hall, E. *Liq. Cryst.* **1993**, *13*, 233−245.
(40) Kannan, R. M.; Rubin, S. F.; Kornfield, J. A. *J. Rheol.* **1994**, *38*, 1609−1622.
(41) Kannan, R. M.; Kornfield, J. A.; Schwenk, N.; Boeffel, C. *Adv. Mater.* **1994**, *6*, 214−216.
(42) Rubin, S. F.; Kannan, R. M.; Kornfield, J. A.; Boeffel, C. *Macromolecules* **1995**, *28*, 3521−3530.
(43) Berghausen, J.; Fuchs, J.; Richtering, W. *Macromolecules* **1997**, *30*, 7574−7581.
(44) Gu, D.-F.; Jamieson, A. M. *Macromolecules* **1994**, *27*, 337−347.
(45) Yao, N.; Jamieson, A. M. *J. Rheol.* **1998**, *42*, 603−619.
(46) Yao, N.; Jamieson, A. M. *Macromolecules* **1998**, *31*, 5399−5406.
(47) Grabowski, D.; Schmidt, C. *Macromolecules* **1994**, *27*, 2632−2634.
(48) Siebert, H.; Grabowski, D.; Schmidt, C. *Rheol. Acta* **1997**, *36*, 618−627.
(49) Schmidt, C.; Becker, P.; Hasenhindl, A.; Müller, S. In *Progress and Trends in Rheology V, Proceedings of the Fifth European Rheology Conference*; Emri, I., Cvelbar, R., Eds.; Steinkopff: Darmstadt, 1998; pp 238−239.
(50) Siebert, H. Ph.D. Thesis, Universität Freiburg, 1998.
(51) Quijada-Garrido, I.; Siebert, H.; Becker, P.; Friedrich, C.; Schmidt, C. *Rheol. Acta* **1999**, *38*, 465−502.
(52) Quijada-Garrido, I.; Siebert, H.; Schmidt, C.; Friedrich, C. In *Progress and Trends in Rheology V, Proceedings of the Fifth European Rheology Conference*; Emri, I., Cvelbar, R., Eds.; Steinkopff: Darmstadt, 1998; pp 236−237.
(53) Finkelmann, H.; Rehage, G. *Makromol. Chem. Rapid Commun.* **1980**, *1*, 31−34.
(54) Disch, S.; Schmidt, C.; Finkelmann, H. *Makromol. Chem. Rapid Commun.* **1994**, *15*, 303−310.
(55) Maffettone, P. L.; Marrucci, G.; Mortier, M.; Moldenaers, P.; Mewis, J. *J. Chem. Phys.* **1994**, *100*, 7736−7743.

MA991490M